

University of Groningen

Position-history and spin-history artifacts in fMRI time-series

Muresan, Lucian; Renken, Remco; Roerdink, Jos B.T.M.; Duifhuis, Hendrikus

Published in:
EPRINTS-BOOK-TITLE

IMPORTANT NOTE: You are advised to consult the publisher's version (publisher's PDF) if you wish to cite from it. Please check the document version below.

Document Version
Publisher's PDF, also known as Version of record

Publication date:
2002

[Link to publication in University of Groningen/UMCG research database](#)

Citation for published version (APA):

Muresan, L., Renken, R., Roerdink, J. B. T. M., & Duifhuis, H. (2002). Position-history and spin-history artifacts in fMRI time-series. In EPRINTS-BOOK-TITLE University of Groningen, Johann Bernoulli Institute for Mathematics and Computer Science.

Copyright

Other than for strictly personal use, it is not permitted to download or to forward/distribute the text or part of it without the consent of the author(s) and/or copyright holder(s), unless the work is under an open content license (like Creative Commons).

Take-down policy

If you believe that this document breaches copyright please contact us providing details, and we will remove access to the work immediately and investigate your claim.

Downloaded from the University of Groningen/UMCG research database (Pure): <http://www.rug.nl/research/portal>. For technical reasons the number of authors shown on this cover page is limited to 10 maximum.

Position-history and spin-history artifacts in fMRI time-series

Lucian Muresan^a, Remco Renken^b, Jos B.T.M. Roerdink^a, Hendrikus Duifhuis^b

^a University of Groningen, Institute for Mathematics and Computing Science

^b University of Groningen, Biomedical Engineering

ABSTRACT

What is the impact of the spin history and position history on signal intensity after the alignment of acquired volumes? This question arises in many fMRI studies. We will focus on spin-history artefacts generated by the position-history of the scanned object. In fMRI an object is driven to steady state by applying a few dummy scans at the start of each measurement. A change in object position will disrupt the tissue's steady state magnetization. The disruption will propagate to the next few acquired volumes until a steady state is reached again. The variables which are involved in changing the longitudinal magnetization are: the shape and the position of the slice profiles, the times at which RF pulses occurred, the equilibrium magnetization map and the T_1 map. Knowledge of these variables enables the prediction of those situations and the locations where the spin-history may compromise the fMRI analysis. In this paper we present a simulation of spin-history artefacts. The simulation shows that these effects, following a displacement, are similar to the transient period at the beginning of the measurement. Introducing gaps between the acquired slices increases these artefacts.

Keywords: artefacts, fMRI, position-history, spin-history, steady state

1. INTRODUCTION

Functional magnetic resonance imaging (fMRI) tries to identify brain areas involved in executing a specific task. These brain areas are identified using the Blood Oxygen Level Dependant (BOLD) effect. Upon activation oxygenation levels of blood change locally in the brain. This effect is very small generating only 1-5% signal changes at the most common magnetic field strength (1.5 T). Other processes, which induce changes of the same order of magnitude or more, can compromise the final statistical tests. One such a process is the effect of motion via spin-history on the signal intensity. We will present a simulation that allows us to estimate the magnitude and location of these effects. Any signal modulation not related to the BOLD effect is normally treated as noise in fMRI. A description of the impact of noise on interpretation of fMRI data can, for example, be found in Parrish et al.¹ They describe a method that allows the quantitative and qualitative comparison of fMRI imaging methods based on the signal to noise ratio (SNR). An experimental study of different sources of noise in fMRI can be found in Zarahn et al.,² Aguirre et al.³ Head motion is one of the main sources of noise in fMRI. Depending on (1) the time at which the change in head position occurs, (2) the imaging sequence used, (3) the type of motion, (4) the amplitude of motion, (5) the interpolation scheme, different correction algorithms have been proposed. The majority of techniques use retrospective motion correction. Time series data are processed after all the data has been acquired.⁴⁻⁶ Another technique, known as prospective acquisition correction, updates imaging sequence parameters based on the previously acquired volumes. In this way, influences of through-plane motion on the history of magnetization is minimized.⁷⁻⁹ The retrospective and prospective methods mentioned above only correct for motion that occurs between the acquisition of volumes. If a change in position occurs between acquisition of two slices (i.e. during the acquisition of a volume), a realignment of the slice stacks can be used to correct for the motion.¹⁰ Motion during the acquisition of Fourier data is assumed to be negligible when using fast imaging techniques such as echo planar imaging (EPI).

Further author information:

L. M.: E-mail: lucian@cs.rug.nl

In this paper we will focus on head motion during the interval between two successive volume acquisitions, which is the most common type of head motion in fMRI. The primary effect of the movement is the change of head position in the scanner reference system (SRS). The series of positions of the object during the experiment defines its position-history. For the MRI scanner the scanned object is a system of magnetic spins, e.g. in water protons. The magnetic properties of this system during acquisition define the final output image. There are several mechanisms which influence the magnetic state of the scanned object through changes in position. One is via the main B_0 magnetic field irregularities. Irregularities arise from imperfections in the B_0 field and magnetic susceptibility of the object. Shimming is established only once, in order to counter these effects, prior to each measurement. It is not recalculated for each volume acquisition. In fact each new position requires a new shimming. These susceptibility induced artefacts are difficult to correct.

Another way to change the magnetic state is via the geometry of excitation profiles. The positions of the excitation profile are designed in the SRS. Usually they are parallel and equidistant to each other. A new position of the object involves a new position of the excitation profiles relative to the object reference system (ORS). Thus the excitation profiles will have a different impact on the magnetic state of the system. If the spin system has no time to return to equilibrium before the next excitation pulse occurs, the magnetic state of the system will depend on the history of past magnetic states. This motion-related effect is known as spin history.⁶ Furthermore motion-related effects, not related to the magnetic properties of the object, are generated by interpolation procedures used for realignment.¹¹

If there is a correlation between the task and the movement, these changes can be confused with those due to the BOLD effect.¹² If there is no correlation between the task and movement an increase of the variance in fMRI signal will still occur. This will also result in a reduced detectability of the BOLD effect. The spin history problem was formulated by Friston et al.⁶ They also proposed to reduce the intensity changes by regressing the data against the movement time series derived from the registration procedure.⁶ It is unclear under what circumstances (e.g. amplitude and type of motion, RF sequence, T_1 properties) this spin-history has a profound effect on signal analysis.

This paper investigates intensity artefacts introduced by spin history via position history. We focus on the following questions: (1) does the set of the parameters, used for acquiring the data, give rise to a spin-position-history artefact?; (2) in which voxels can a modulation of the intensity generated by a spin-position-history effect be expected?

2. DESCRIPTION OF THE MECHANISM

RF pulses and gradients sequences are designed assuming that the scanner reference system (SRS) and the object reference system (ORS) will have the same relative position during the entire measurement. The spin history is influenced by the slice profile (flip angle profile) in the object reference system. Each RF pulse has a corresponding flip angle spatial map $\alpha(x, y, z)$ in the scanner reference system. In the object reference system this map may rotate or translate if the scanned object is rotated or translated (see Fig.1). Thus the change in the position of the scanned object influences the spin history via the flip angle profile. Some of the motion correction algorithms which focus on the alignment of the slice stacks¹⁰ do not take this spin-history effect into account. Inter-slice motion generates overlapped slice profiles, see Fig.1. The overlapping regions are subject to a double excitation in a very short interval. This will have an effect that is similar to cross-talk. In the case of cross-talk the overlapping is due to the improper choice of the distance between successive slice excitation profiles. Changing the order of slice acquisition the cross-talk can be reduced. This is also true for the spin-history in case of interslice motion.

If there is no motion during acquisition of the volumes, but there is between acquisition of two successive volumes, then the spin-history can be changed by the position history. If all the regions of the object are in magnetic equilibrium prior to each volume acquisition, there will be no spin history effect. In most fMRI experiments only the first volume acquired is at equilibrium magnetization; all subsequent acquired volumes are not. Because the spins are excited periodically and relatively rapidly, they do not return to equilibrium, but reach a certain (non-equilibrium) steady state.¹⁵ Normally a few dummy scans are recorded to drive the system to this steady state. These dummy scans (usually two or three) are discarded from the further

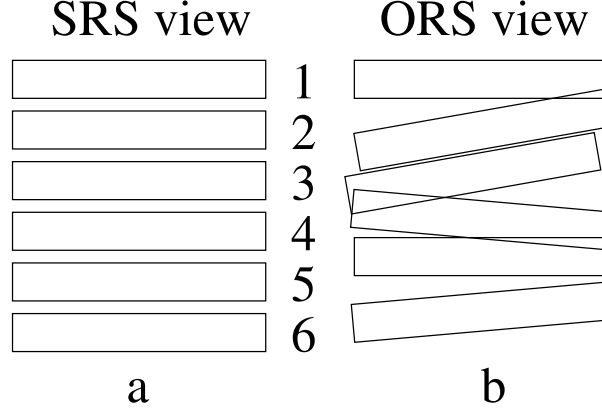


Figure 1. The position of six slice profiles viewed in scanner reference system (SRS) and in scanned object reference system (ORS) in the case the object changes the position in between two slice acquisitions. Inter-slice motion generates overlapped slice profiles which will have the similar impact on the final image as cross-talk effect.

processing because they contain a very intense spin history modulation. The steady state of the scanned object is maintained as long as the periodicity of the RF excitations and gradients are maintained in ORS. A change in position relative to the slice profiles will destroy this periodicity. Thus a transition period toward a new steady state will occur. The transient state can last for several volumes after the displaced volume. The intensity of the signal in those volumes will change during this transition.

3. THEORY

The spin history of the scanned object is influenced by: (1) position and shape of the slice excitation profiles, (2) the times at which RF pulses occur, (3) the set of positions of the scanned object for each slice acquisition, and (4) the equilibrium magnetization and relaxation time maps (that is, their spatial distribution). This section will focus on the description of the behavior of longitudinal magnetization (M_z) of a small part (dV) of the scanned object. The two main parameters for this volume are the relaxation time (T_1) and the equilibrium magnetization (M_{eq}) in the static magnetic field (B_0). We will use the following notations:

- A set of all (N) flip angle maps ($\alpha_1(\vec{r}), \dots, \alpha_N(\vec{r})$). The flip angle for each position \vec{r} in the SRS is defined by the shape of the RF pulses, together with the applied strength of the slice selection gradient.
- The times at which RF pulses occur: t_1, \dots, t_N .
- The z-axis is oriented along the main magnetic field B_0 .
- For the small volume under consideration there is a set of positions $\vec{R}_1, \dots, \vec{R}_N$ at times t_1, \dots, t_N . This set defines the position-history for the given part dV . By knowing the position of the entire rigid object it is possible to get this set of positions for every small volume of the scanned object. The motion can have components both parallel or perpendicular to the longitudinal axis Oz.
- The initial z-magnetization of the considered part : $M_0 = M_{eq}$.
- The longitudinal relaxation time of the considered part: T_1 .

In this work we use the following conditions:

- The acquisition of one slice is based on one RF pulse (e.g. an EPI sequence).

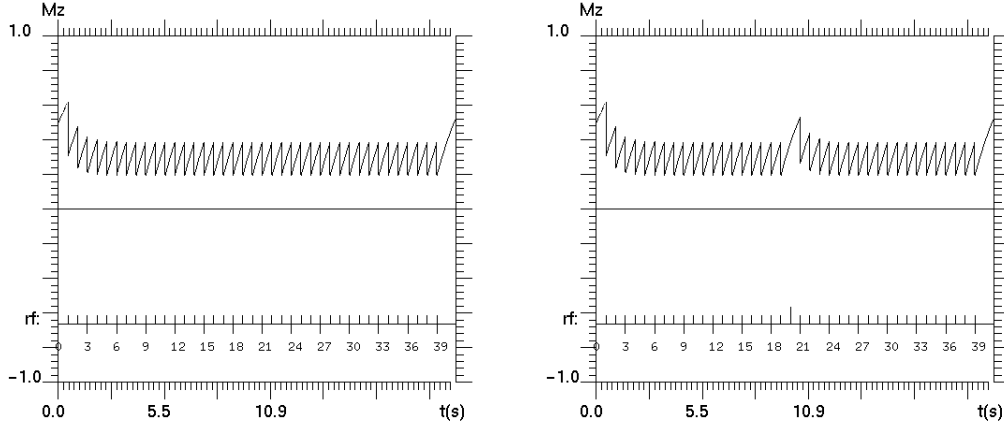


Figure 2. Behavior of the longitudinal magnetization of the small part dV during scanning. Shown is the behavior of M_z when there were no changes in position (left) and in the case when at 20th RF pulse a back and forth motion occurred. There is a temporary disruption of the steady state. The small part dV will “feel” the effect of each RF pulse depending on the position of dV relative to the flip-angle map of that RF pulse. The following sequence of flip-angles will influence the state of the magnetization of dV : $\alpha_1(\vec{R}_1)$, $\alpha_2(\vec{R}_2)$... $\alpha_N(\vec{R}_N)$. At each time an RF pulse occurs we have discontinuities in longitudinal magnetization.

- The change in position occurs between acquisitions of two successive slices or two successive volumes. So possible motion during the acquisition of one slice is neglected.
- The intensity of the acquired image will be proportional to the transversal component M_{xy} immediately after the RF pulse.
- We explicitly do not take into account other effects that could result from a displacement, like shimming effects, interpolation approximations, susceptibility effects and non-uniformity of B_0 .

The impact of the k^{th} RF pulse on the magnetization of dV will depend on its relative position with respect to excitation profile $\alpha_k(\vec{r})$. At $t=0$, dV is inside the scanner at position \vec{R}_1 . The first RF pulse occurs at $t_1 = 0$ and will tilt the magnetization vector over a certain flip angle described by the flip-angle map of that pulse $\alpha_1(\vec{r})$. In our small volume the flip angle will be $\alpha_1(\vec{R}_1)$. The longitudinal magnetization M_1^b immediately before this RF pulse is the equilibrium magnetization. $M_1^b = M_{eq}$. And the longitudinal magnetization M_1^a immediately after this RF pulse is

$$M_1^a = M_1^b \cos(\alpha_1(\vec{R}_1)). \quad (1)$$

The corresponding transversal magnetization M_{xy} immediately after this RF pulse is

$$M_{xy1}^a = M_1^b \sin(\alpha_1(\vec{R}_1)). \quad (2)$$

The intensity of this point in the image will be proportional to this transversal magnetization M_{xy1}^a . The longitudinal magnetization $M_z(t)$ between the first pulse and the second ($t_1 < t < t_2$) is

$$M_z(t) = M_{eq}(1 - e^{-\frac{t-t_1}{T_1}}) + M_1^a e^{-\frac{t-t_1}{T_1}}; \quad t \in (t_1, t_2). \quad (3)$$

At the second RF pulse, the position of dV will be \vec{R}_2 . At $t = t_2$ but immediately before the second RF pulse, the M_z magnetization is

$$M_2^b = M_{eq}(1 - e^{-\frac{t_2-t_1}{T_1}}) + M_1^a e^{-\frac{t_2-t_1}{T_1}}. \quad (4)$$

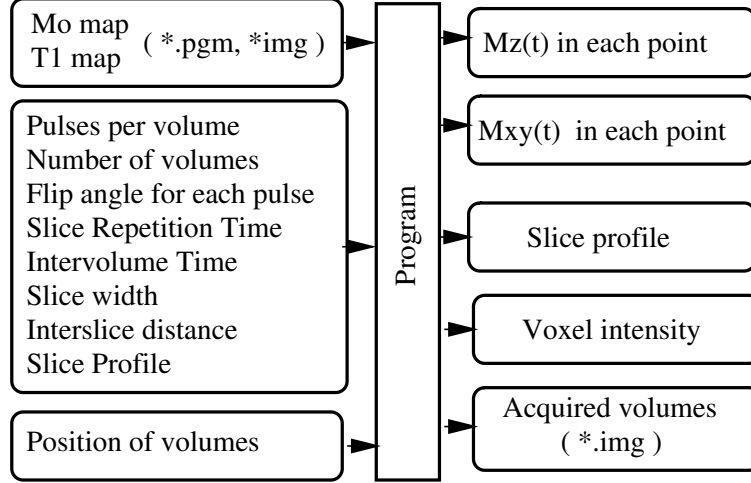


Figure 3: The input and output of the spin history-motion history simulator.

We can apply this method iteratively for all RF pulses and corresponding positions of dV . Now the equations for the k^{th} pulse are as follows. Immediately after k^{th} RF pulse the longitudinal magnetization M_k^a is

$$M_k^a = M_k^b \cos(\alpha_k); \quad k = 1, 2, \dots, N. \quad (5)$$

Immediately before k^{th} RF pulse the longitudinal magnetization M_k^b is

$$M_k^b = M_{eq} \left(1 - e^{-\frac{t_k - t_{k-1}}{T_1}} \right) + M_{k-1}^a e^{-\frac{t_k - t_{k-1}}{T_1}} \quad k = 2, \dots, N. \quad (6)$$

Between k^{th} and $(k+1)^{th}$ RF pulse the magnetization $M_z(t)$ is

$$M_z(t) = M_{eq} \left(1 - e^{-\frac{t - t_k}{T_1}} \right) + M_k^a e^{-\frac{t - t_k}{T_1}}; \quad t \in (t_k, t_{k+1}) \quad k = 1, 2, \dots, N-1. \quad (7)$$

The equations (5- 7) define the behavior of M_z in each point of the object. Starting with magnetic equilibrium, application of a periodic RF sequence to the same part of the scanned object will drive M_z into a steady state (Fig.2, left panel). There will be a transition period from the equilibrium to the steady state. This is why in fMRI experiment the first few acquired volumes are discarded. A change in position will destroy the steady state producing a temporary transition state (Fig.2, right panel).

4. SIMULATION RESULTS: TEMPORARY DESTRUCTION OF THE STEADY STATE

In order to be able to visualize the effects of both position history and spin history we implemented the equations (5)-(7) into a simulation program. The main issue we focused on is the destruction of the steady state by a displacement of the object. The displacement can modify the intensity of the next few volumes, even if those volumes are not displaced themselves during the experiment. The impact of motion on the steady state depends on many parameters. These are the input of the simulation program (Fig.3).

The 3D input maps of M_0 and T_1 can be generated from gray PGM images or from an Analyze file. The position along z -direction (perpendicular to the slice plane) of the scanned object is defined for each RF pulse. The slice geometry is described by: the position of the center of the slice, the slice width and its shape. The interslice repetition time and inter-volume repetition time define when the RF pulses occur.

In the simulations we used the following values:

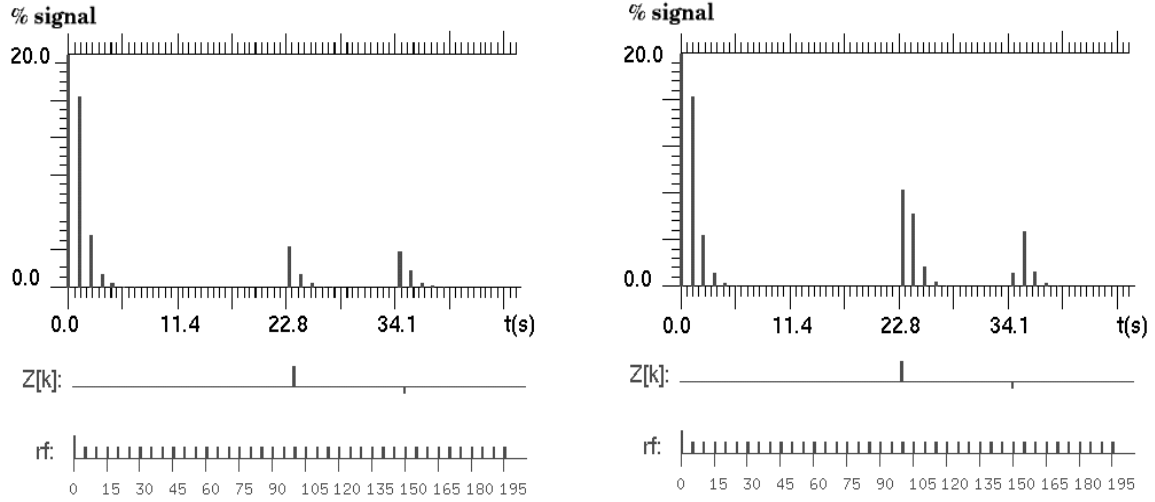


Figure 4. Comparison of the effect on steady state when no gap (left) and a gap between slices (right) is present. If there is a change in position the geometry of the relative position of the slice profiles will influence the amount of disruption of the steady state. The voxel has $T_1=1.9$ seconds. There are three transition periods.

- equilibrium magnetization: $[0, 1]$ interval.
- T_1 : $[0.5, 3]$ seconds interval.
- in plane grid: 64×64 voxels.
- slice profile: rectangular.
- distance between the centers of the slices: 1mm
- number of slices per volume: 5
- number of volumes: 40
- flip angle: 60 degree s
- interval between acquisition of two successive slices: 0.03 s
- interval between the end of a volume and beginning of the next volume: 1 s (thus $TR=1.1$ s)
- the density of object points in the z -direction: 20 points per mm.
- the order of slice acquisition: sequential.

In figure 4 the relative intensity $100 \frac{|I_k - I_{10}|}{I_{10}}$ ($k=1, 2, \dots, 40$) of a voxel is shown. The 10th volume is chosen as reference because the object has reached steady state at this point. We applied two back-and-forth motions; the 20th volume was displaced by $+0.3$ mm and the 30th volume was displaced by -0.1 mm. All the other volumes were at the starting position. Slice width was either 1 mm (no gap Fig.4 left) or 0.8mm (with a gap of 0.2mm Fig.4 right). Each change in the position triggers a transient behavior. Note the similarity between its shape and the initial couple of volumes, where the system is driven to steady state. Without a motion correction the

signal from the displaced volume belongs to another part of the scanned object. Here we concentrate on the following volumes which have returned to the original position.

The first few volumes in an fMRI time-series are discarded because of the presence of non-steady state. What about volumes 20, 21 and 22 or volumes 30, 31, 32 ? The volumes 21, 22 did not change the position at all but they do contain a spin-history modulation propagated from the displaced 20th volume. There is a similar disruption of the steady state in volumes 31 and 32 generated by the displacement of 30th volume. When there is a gap between slice profiles the destruction of the steady state is more pronounced, see Fig. 4. The effect is stronger and lasts longer; volumes 23 and 33 also contain spin-history modulation. The rate of returning to steady state after a displacement depends on many factors like T_1 and flip angle. On average, two to four volumes after the displacement will be affected.

In this example, the amplitude of the spin-history modulation in the case with no gaps can reach up to 3% of the steady state intensity. The presence of the gaps increases this amplitude to 7%. These results show that the simulation program allows us to predict the location and amplitude of the spin-history artifacts.

5. CONCLUSION

At the very beginning of an fMRI measurement the scanned object enters into steady state starting from equilibrium; these first few dummy volumes are discarded. The steady state depends on the position of the scanned object relative to the position of the slice profiles. The position-history is responsible for the spin-history effect. A new position of the scanned object means a new steady state associated to that position. A change in position generates a new steady state of the scanned system. The migration from one steady state to another takes time. In that transition period the intensity of the signal may vary in a range comparable to that generated by the BOLD effect. The slices acquired at the edges of the volume are often discarded because a change in position has a high impact on the steady state at that position. A gap between slices creates a situation which is similar to that at the margins of the scanned area. The disruption of the steady state is much higher when a gap is present.

In this paper we investigated how motion destroys the steady state magnetization of a scanned object in a fMRI framework. We presented an example of back and forth motion of the object for the duration of one volume acquisition. This back and forth motion destroyed the steady state. This effect lasted for several subsequent volumes. The period during which the system is not in steady state behaves similar to the transient period at the beginning of the measurement. The amplitude of the spin-history effect in the non-steady state was in the order of 3% to 7%. The changes in intensity and the duration of the non-steady state are influenced by the local T_1 , the flip angle, the slice width, the slice profile, the gap width, the slice excitation order, and the amplitude of motion.

After the realignment of the time series the position-history of each acquired volume is known. The first few volumes allow the estimation of the T_1 and M_0 maps. With this information the simulation program we developed is able to predict the location and estimate the amplitude of the spin-history modulation generated by the changes in position. Once the spin-history modulation is known its related artefacts can be removed from the data. Future work will focus on the development of a T_1 phantom which can be displaced in a controlled fashion inside the scanner. Using this phantom we will further investigate how position-history influences the spin-history, and develop algorithms for correcting the corresponding artefacts.

REFERENCES

1. T. B. Parrish, D. R. Gitelman, K. S. LaBar, M. M. Mesulam, "Impact of Signal-to-Noise on Functional MRI", *Magn. Reson. Med.* **44**, pp. 925–932, 2000.
2. E. Zarahn, G. K. Aguirre, M. D'Esposito, "Empirical Analyses of BOLD fMRI Statistics, I. Spatially Unsmoothed Data Collected under Null-Hypothesis Conditions", *Neuroimage* **5**, pp. 179–197, 1997.
3. G. K. Aguirre, E. Zarahn, M. D'Esposito, "Empirical Analyses of BOLD fMRI Statistics, II. Spatially Unsmoothed Data Collected under Null-Hypothesis Conditions", *Neuroimage* **5**, pp. 199–212, 1997.

4. K. J. Friston, A. P. Holmes, J. B. Poline, et al, "Analysis of fMRI time-series revisited", *Neuroimage* **2**, pp. 45–53, 1995.
5. K. J. Friston, P. Jezzard, R. Turner, "Analysis of Functional MRI Time-Series", *Human Brain Map* **1**, pp. 153–171, 1994.
6. K. J. Friston, S. Williams, R. Howard, R. S. Frackowiak, R. Turner, "Movement-related effects in fMRI time-series" *Magn. Reson. Med.* **35**, pp. 346–355, 1996.
7. S. Thesen, O. Heid, E. Mueller, L. R. Schad, "Prospective Acquisition Correction for Head Motion With Image-Based Tracking for Real-Time fMRI", *Magn. Reson. Med.* **44**, pp. 457–465, 2000.
8. C. C. Lee, R. C. Grimm, A. Manduca, J. P. Felmlee, R. L. Ehman, S. J. Riederer, C. R. Jack, "A prospective approach to correct for interimage head rotation in fMRI", *Magn. Reson. Med.* **39**, pp. 234–243, 1998.
9. H. A. Ward, S. J. Riederer, R. C. Grimm, et al., "Prospective multiaxial motion correction for fMRI", *Magn Reson Med* **43**, pp. 459–469, 2000.
10. B. Kim, J. L. Boes, P. H. Bland, T. L. Chenevert, C. R. Meyer, "Motion Correction in fMRI via Registration of Individual Slices Into an Anatomical Volume", *Magn. Reson. Med.* **41**, pp. 964–972, 1999.
11. S. Grootenboer, C. Hutton, J. Ashburner, A. M. Howseman, O. Josephs, G. Rees, K. J. Friston, R. Turner, "Characterization and Correction of Interpolation Effects in the Realignment of fMRI Time Series", *NeuroImage* **11**, pp. 49–57, 2000.
12. J. V. Hajnal, R. Myers, A. Oatridge, J. E. Schwieso, I. R. Young, G. M. Bydder, "Artifacts due to stimulus correlated motion in functional imaging of the brain", *Magn. Reson. Med.* **31**, pp. 283–291, 1994.
13. M. D. Robson, J. C. Gatenby, A. W. Anderson and J. C. Gore, "Practical considerations when correcting for movement-related effects present in fMRI time-series", *Proc. ISMRM 5th Annual Meeting*, Vancouver, pp. 1681, 1997.
14. V. L. Morgan, D. R. Pickens, S. L. Hartman, R. R. Price, "Comparasion of Functional MRI Image Realignment Tools Using a Computer-Generated Phantom", *Magn. Reson. Med.* **46**, pp. 510–514, 2001.
15. A. B. Hargreaves, S. S. Vasanawala, M. J. Pauly and G. D. Nishimura, "Characterization and Reduction of the Transient Response in Steady-State MR Imaging", *Magn. Reson. Med.* **46**, pp. 149–158, 2001.